



HAL
open science

Interference with energy metabolism by 5-aminoimidazole-4-carboxamide-1-beta-D-ribofuranoside induces HPV suppression in cervical carcinoma cells and apoptosis in the absence of LKB1

Julia Nafz, Johanna De-Castro Arce, Verena Fleig, Andrea Patzelt, Sybille Mazurek, Frank Rösl, Frank Rösl

► To cite this version:

Julia Nafz, Johanna De-Castro Arce, Verena Fleig, Andrea Patzelt, Sybille Mazurek, et al.. Interference with energy metabolism by 5-aminoimidazole-4-carboxamide-1-beta-D-ribofuranoside induces HPV suppression in cervical carcinoma cells and apoptosis in the absence of LKB1. *Biochemical Journal*, 2007, 403 (3), pp.501-510. 10.1042/BJ20061053 . hal-00478629

HAL Id: hal-00478629

<https://hal.science/hal-00478629>

Submitted on 30 Apr 2010

HAL is a multi-disciplinary open access archive for the deposit and dissemination of scientific research documents, whether they are published or not. The documents may come from teaching and research institutions in France or abroad, or from public or private research centers.

L'archive ouverte pluridisciplinaire **HAL**, est destinée au dépôt et à la diffusion de documents scientifiques de niveau recherche, publiés ou non, émanant des établissements d'enseignement et de recherche français ou étrangers, des laboratoires publics ou privés.

Interference with energy metabolism by 5-aminoimidazole-4-carboxamide-1- β -D-ribofuranoside induces HPV suppression in cervical carcinoma cells and apoptosis in the absence of LKB1

Julia Nafz, Johanna De-Castro Arce, Verena Fleig, Andrea Patzelt, Sybille Mazurek¹⁾ and Frank Rösl*

Angewandte Tumorstudiologie, Abteilung Virale Transformationsmechanismen, Deutsches Krebsforschungszentrum, Heidelberg, Germany

¹⁾Institut für Biochemie und Endokrinologie, Fachbereich Veterinärmedizin, Universität Giessen, Germany

Running title: Effects of AICAR on HPV-positive cells

Key words: HPV transcription, AP-1; AMPK; p53; therapy.

Abbreviations

AICAR: 5-aminoimidazole-4-carboxamide-1- β -D-ribofuranoside

AMPK: AMP dependent kinase

ACC: acetyl-CoA-carboxylase

PRPP: 5-phospho-D-ribosyl-1-pyrophosphate

PARP: poly (ADP-ribose) polymerase

***Corresponding author:**

Prof. Dr. Frank Rösl

Angewandte Tumorstudiologie

Abteilung Virale Transformationsmechanismen

Deutsches Krebsforschungszentrum

Im Neuenheimer Feld 242

D-69120 Heidelberg

Tel. ++49-6221-42-4900

Fax++49-6221-42-4902

e-mail: f.roesl@dkfz.de

Synopsis

Carcinogenesis is a dynamic and stepwise process, which is accompanied by a variety of somatic and epigenetic alterations in response to a changing microenvironment. Hypoxic conditions will select for cells, which have adjusted their metabolic profile and maintain proliferation by successfully competing for scarce nutritional and oxygen resources. In the present report we have studied the effects of energy depletion in the context of HPV-induced pathogenesis. We show that cervical carcinoma cell lines are susceptible to undergo either growth arrest or cell death under conditions of metabolic stress induced by 5-aminoimidazole-4-carboxamide-1- β -D-ribofuranoside (AICAR), a known activator of the AMP-activated protein kinase (AMPK). Our results revealed that AICAR treatment led to a reduced binding affinity of the transcription factor AP-1 and in turn to a selective suppression of HPV transcription. Moreover, the outcome of AICAR on proliferation and survival was dependent on p53 activation and the presence of LKB1, the major upstream kinases of AMPK. Using non-malignant LKB1 expressing somatic cell hybrids, which lose expression after tumourigenic segregation as well as siRNA LKB1 knock-down approaches, we could further demonstrate that expression of LKB1 protects cells from cytotoxicity induced by agents which modulate the ATP:AMP ratio. Since simulation of low energy status can selectively eradicate LKB1 negative cervical carcinoma cells, AICAR may represent a novel drug in the treatment of cervical cancer.

INTRODUCTION

Cervical cancer is a sexually transmitted disease with an apparent causal relationship between the infection with certain “high-risk” human papillomavirus types (mostly HPV-16, but also HPVs 18, 33, 45 and some others) and the onset of tumour formation [1]. While the multi-step process of virus-induced carcinogenesis can be mimicked in part under tissue culture conditions [2], accumulation of malignant cells in a patient represents a more complicated constellation, which is determined by the three dimensional environment, depending on external parameters such as blood vessel formation, nutritional supplementation, growth hormones and oxygen [3]. To compensate initial poor vascularisation and low nutritional supply, transformed cells have to adapt to their new surroundings through a profound change in their energy metabolism [3]. Indeed, many tumours including cancer of the *cervix uteri* are characterized by an increased anaerobic catabolism of glucose as energy source [4]. Furthermore, glycolytic intermediates are used as precursors for synthetic processes, debranching from glycolysis such as nucleic acid, phospholipid and amino acid synthesis [5; 6].

Although the glycolytic phenotype seems to be disadvantageous, yielding 18 times less ATP than oxidative phosphorylation [5], its maintenance in primary and metastatic malignancies has a quite obvious selective benefit: cells, which shift to anaerobic glycolysis not only survive the hypoxic microenvironment, but also select for a phenotype resistant to acid-induced toxicity, caused by secretion of lactic acid during incomplete glucose metabolism [3]. Likewise, chronic acidification can even promote invasion of formerly premalignant cells since adjacent normal populations, which are sensitive to acidosis are destroyed [3]. Consequently, fully transformed cells have undergone genetic mutations to an extent that they have partly lost their flexibility to respond to changing conditions such as deprivation of glucose, which makes them susceptible to drugs interfering with energy metabolism [7].

HPV-positive cells, derived from highly invasive cancers depend mainly on glycolysis for energy production [8]. In several studies including animal models, interference with glycolysis by particular inhibitors or glucose withdrawal disturbs the proliferation of tumour cells [9; 10]. In our previous study we have shown that the glucose availability as energy source is not only advantageous for an increased metabolism, but seems to be even indispensable to maintain HPV-18 oncogene transcription in cervical carcinoma cells. This was mainly deduced from the fact that the glucose analogue 2-deoxyglucose (2-DG) was able to suppress viral expression at the level of initiation of transcription. Moreover, 2-DG restored

the normal half-life of the tumour suppressor p53, in response to viral E6/E7 oncogene suppression [11].

Besides a general inhibitory effect on protein glycosylation [12], 2-DG also reduces the intracellular ATP level and in turn increases AMP. Alteration of the intracellular ATP:AMP ratio as a consequence of nutrient starvation or hypoxia usually activates the AMP-activated protein kinase (AMPK), a metabolic stress-sensing protein, which attracted increasing attention in cancer research due to its central role in controlling energy consumption and cell proliferation [13]. AMPK represents a multi-component enzyme complex, which switches off, once activated, many ATP-utilizing processes to sustain energy homeostasis [13]. AMP binding allosterically activates AMPK, facilitating the binding of upstream kinases, which enhance its activity. 5-aminoimidazole-4-carboxamide-1- β -D-ribofuranoside (AICAR), an adenosine analogue has been shown to mimic AMP once phosphorylated to ZMP by adenosine kinase [14]. Its effect on survival of cells depends strongly on cell type and concentration used and varies from induction of growth arrest, prolonged survival, induction of senescence and apoptosis [15]. Moreover, AICAR can even induce apoptosis without AMPK activation [16], which is evidently causally linked with the absence of LKB1, a serine/threonine tumour suppressor kinase, which normally phosphorylates AMPK [17].

In the present report we describe the effects of cellular metabolic stress on HPV-positive cervical carcinoma cells. We show that both viral transcription and cellular growth were strongly affected by AICAR treatment. Notably, the final outcome of the biological response upon AICAR application was determined by the AMPK upstream kinase LKB1 whose expression protects non-malignant HPV-positive cells from apoptosis, while LKB1 negative cells were eliminated. This may open new strategies in the treatment of cervical cancer, using LKB1 expression as predictor for the therapeutic success.

MATERIAL AND METHODS

Cell lines and somatic cell hybrids. The cervical carcinoma cell lines HeLa, SiHa, CaSki, SW756, C33a, the non-tumourigenic somatic cell hybrid (referred to as "444") of HeLa and primary human lung fibroblasts, its tumourigenic segregant (referred to as "CGL3") [18], β -"444", the lung carcinoma cell line H1299 and the chronic myelogenous leukaemia cell line K562 were maintained in Dulbecco's modified Eagle's medium (DMEM, Sigma, München, [11] (Invitrogen, Karlsruhe, Germany)). β -"444" cells were generated by stable transfection of "444" cells with a β -actin promoter driven E6/E7 transcription cassette, representing a viral-cellular chimeric cDNA isolated from SW756 cells. AICAR, 2-DG and uridine (all from Sigma, München, Germany) were dissolved in sterile water. Usually, 2×10^4 cells per cm^2 of the respective cell lines were seeded, and left 24 h before treatment.

RNA extraction and Northern Blot. Cytoplasmic RNA was extracted according to the guanidinium-thiocyanate method or using RNeasy RNA purification kit (Qiagen, Hilden, Germany). 5 μg of total cellular RNA were separated on 1% agarose gels in the presence of ethidium bromide under non-denaturing conditions and transferred to nylon membranes (GeneScreen, NEN Life Science, Köln, Germany). The filters were subsequently hybridized under stringent conditions with specific ^{32}P -labeled DNA probes [11].

DNA hybridization probes. pHPV-16/18 represent the unit-length genome of HPV-16/18 DNA cloned in pBR322. pHF- β A1 harbours an approximately full-length insert of the fibroblast β -actin gene. All probes were labelled by random-priming in the presence of ^{32}P -dCTP [11].

Reverse Transcription and PCR. For reverse transcription, 2 μg of DNase purified RNA was mixed with 0.2 μg of random primers (Roche, Mannheim, Germany), heated at 70°C for 10 min, and chilled on ice. After the annealing, the mixture was supplemented with reaction buffer (50 mM Tris-HCl, pH 8.3, 75 mM KCl, 3 mM MgCl_2), 10 mM dithiothreitol, 500 μM deoxynucleoside triphosphate mixture (Invitrogen, Karlsruhe, Germany) and incubated at 25°C for 10 min. 100 Units of reverse transcriptase SuperScript II (Invitrogen, Karlsruhe, Germany) was added, the reaction was incubated at 42°C for 50 min, heated to 70°C for 15 min, and refrigerated at -20°C until used. PCRs were performed in a solution containing 20 mM Tris-HCl (pH 8.4), 50 mM KCl, 1.5 mM MgCl_2 , 200 μM deoxynucleoside triphosphate mix (Invitrogen, Karlsruhe, Germany), 40 pM of upstream and downstream primers, 1 Unit of

Taq polymerase (Sigma, München, Germany) and 2 µl of reverse-transcribed product. The amplification was performed in an MJ Research PTC-200 thermal cycler in a total volume of 50 µl. The following primers and conditions were used: p21: 5'-ATGTCAGAACCGGCTGGGGATG-3' and 5'-TTAGGGCTTCCTCTTGGAGAAG-3' located in exon 3 and 4 (product length: 494), 4 min 94°C, 28 cycles of 30 sec at 94°C, 45 sec at 55°C, and 30 sec at 72°C, final extension 10 min at 72°C; p53: 5'-CTGAGGTTGGCTCTGACTGTACCACCATCC and 5'-CTCATTCAGCTCTCGGAACATCTCGAAGCG-3', located in exons 7 and 10 (product length 371), 4 min 94°C, 30 cycles of 30 sec at 94°C, 45 sec at 57°C, and 30 sec at 72°C, final extension 10 min at 72°C; LKB1: located in exons 9 and 10 (product length 314), 5'-ATGGAGTACTGCGTGTGTGG -3' and 5'-CCAGATGTCCACCTTGAAGC- 3', 4 min 94°C, 35 cycles of 30 sec at 94°C, 45 sec at 58°C, and 1 min at 72°C, final extension 10 min at 72°C; GAPDH (internal control):5'-TGGATATTGTTGCCATCAATGACC-3' and 5'-GATGGCATGGACTGTGGTCATG-3' , 4 min 94°C, 25 cycles of 30 sec at 94°C, 45 sec at 65°C, and 30 sec at 72°C, final extension 10 min at 72°C. The PCR products were analyzed in 2% agarose gels containing ethidium bromide.

SDS-PAGE and Western blotting. Total cellular protein extracts were prepared using RIPA buffer (0.5% deoxycholate, 0.5% NP-40, 0.5% SDS, 50 mM Tris pH 7.4 and 100 mM NaCl) supplemented with serine-protease inhibitor phenyl-methyl-sulfonyl-fluoride (PMSF) to a final concentration of 10 µg/ml. Cells were sonified using a Sonifier 250 (Branson Ultrasonics, Geneva, Switzerland) and after removing the cell debris by centrifugation, the supernatant was immediately frozen and kept at -80°C. Nuclear and cytosolic extracts were prepared according to the method of Schreiber et al. [19], adding the protease inhibitors N-N-(L-3-trans-carboxyoxirane-2-carbonyl)-L-leucyl-arginine (E64) and 4-(2-aminoethyl)-benzolsulfonylflouride ("Pefabloc SC") in concentrations suggested by the manufacturer (Roche, Mannheim, Germany). Concentrations of RIPA and nuclear extracts were determined using the Bio-Rad DC Protein Assay Kit (Bio-Rad, München, Germany). 20 µg cellular and 50 µg total protein extracts were separated in 8-12% SDS PAGE, electrotransferred to Immobilon-P membranes (PVDF, Millipore, Bedford, USA) and probed with the following antibodies: human specific murine monoclonal antibody (MAb) directed against p53 (DO1, Santa Cruz, Heidelberg); p21 MAb (Anti Cip/Waf1, BD Transduction Laboratories, Heidelberg); poly (ADP-ribose) polymerase (PARP) MAb (Sc-8007, Santa Cruz, Heidelberg); actin MAb (clone 4, ICN Biomedicals, Meckenheim, Germany); human specific rabbit

antibodies c-Jun (H-79, Santa Cruz 1694, Heidelberg) and phospho-acetyl-CoA carboxylase MAb (p-ACC, Cell Signalling, Frankfurt, Germany). The incubation was carried out overnight at 4°C in Tris-buffered saline (TBS) supplemented with 5% skim milk powder (Sigma, München, Germany), 0.05% Tween 20 (Sigma, München, Germany) and the diluted antibody. The bands were visualized with anti-mouse IgG antibodies conjugated with horseradish peroxidase using the ECL detection system (Amersham-Pharmacia, Freiburg, Germany). For reincubation with additional antibodies, the filters were stripped with 200 mM NaOH for 5 min at room temperature. Equal protein transfer and loading was controlled by reincubation with an actin specific antibody.

Electrophoretic mobility shift assays (EMSA). Oligonucleotides for an HPV-18-specific AP-1-binding site 5'-CGCACCTGGTATTAGTCATTTTCC-3' within the enhancer region, position 7596-7620, the AP-1 consensus sequence 5'-CGCTTGATGACTCAGCCGGAA-3' from the human collagenase promoter [20] and Oct-1 consensus sequences 5'-TGTCGAATGCAAATCACTAGAA-3' derived from the immunoglobulin light chain enhancer [21] were generated in an Applied Biosystems (Foster City, CA, USA) synthesizer and purified by high performance liquid chromatography. The annealed oligonucleotides were labeled with 3000 Ci/mmol [γ -³²P]ATP (Amersham Biosciences, Freiburg, Germany) and T4 polynucleotide kinase (New England Biolabs, Frankfurt a.M., Germany) and gel-purified. Binding reactions were performed in 20 μ l containing 10% glycerol, 12 mM HEPES, pH 7.9, 4 mM Tris-HCl, pH 7.9, 60 mM KCl, 1mM EDTA, dithiothreitol, 0.6 mg/ml bovine serum albumin, 2 μ g of poly(dI-dC), and 2 μ g of nuclear extract. After 5 min, 10000 cpm of the probe was added and incubation was continued for 30 min at room temperature. For super shifts, 2 μ g of either c-Jun (sc-822X), Fra-1 (sc-183X) or c-Fos (sc-52X) are added and incubated for one hour (all antibodies for supershift: Santa Cruz, Heidelberg, Germany). The complexes were resolved with 5.5% non-denaturing polyacrylamide gels (29:1 cross-linking ratio). The gels were dried and exposed to x-ray films (Amersham-Pharmacia, Freiburg, Germany)

Transfection of a HPV-18 URR reporter construct. To circumvent corrections for transfection efficiencies, a luciferase reporter construct under the control of the complete HPV-18 URR was transfected on 1×10^6 HeLa cells in a semistable fashion. In detail, cells were seeded in 6 cm culture dishes for 24 h. The next day, cells were transfected using Effectene reagent (Qiagen, Hilden, Germany) containing 2 μ g of the HPV-18 URR-Luc

plasmid and 0.2 μg of a plasmid carrying a dominant selection marker for neomycin resistance. The cells were first incubated in the absence of the selective antibiotic G-418 (Geneticin). 24 h post transfection, medium was changed and supplemented with 1 mg/ml G-418. The outgrowing clones were pooled and used for luciferase assay. H1299 cells semi-stable transfected with HPV-18 URR-Luciferase construct were kindly provided by Daniela Holland (DKFZ, Heidelberg-Germany) and served as a control for HPV-negative cells. All experiments were performed by triplicate. For the luciferase assay, 6 well plates were seeded with 5×10^5 cells. The next day, 3 wells were supplemented with 4mM AICAR without changing the medium and the remaining 3 wells were used as controls. 24 h after treatment, cells were collected and lysed in passive lysis buffer (Promega, Mannheim, Germany) and luciferase activity was evaluated in a luminometer (Berthold, Bundoora, Australia) using Luciferase Assay Reagent II (Promega, Mannheim, Germany).

siRNA transfection. For knock-down experiments, 75 nM SMARTpool siRNA against LKB1 (Dharmacon, Chicago, USA) was transfected using HiPerFect (Qiagen, Hilden, Germany) according to the instruction of the manual. siRNA directed against the luciferase gene served as negative control. 2×10^6 cells were transfected and seeded in 10 cm plates. The next day, cells were split 1:4 and cultured for additional 24 h. To control the efficiency of the knock-down, cells were collected for RNA preparation using RNeasy kit (Qiagen, Hilden, Germany) according to the manufacturer instructions. RT-PCR was performed to monitor LKB1 expression.

DNA staining, flow cytometry and quantification of apoptosis. Cells including supernatants were harvested by trypsination, washed twice with phosphate-buffered saline (PBS) and fixed overnight with 70% ethanol. After fixation and centrifugation, the cell pellets were resuspended in DNA staining solution containing 5 μM DAPI for DNA and 5 μM SR 101 as a protein counter stain following the protocol published by Stoehr *et al.* [22]. Processing and cell cycle analysis were performed according to Dean and Jett [23] with the cytofluorograph 30-L (Ortho, Raritan, NJ, USA). Cells were additionally analysed by fluorescence microscopy (Leica DMRD, Leitz, Wetzlar, Germany).

RESULTS

Selective down-regulation of HPV transcription in cervical carcinoma cell lines. 2-DG treatment was reported to reduce selectively the transcription of viral mRNA encoding HPV-18 specific oncogenes E6/E7 in HeLa cells concomitant with a decrease in intracellular ATP levels [11]. As subsequently shown, also other conditions of energy deprivation such as hypoxia and low glucose levels have the same effect on HPV gene expression [12]. 2-DG is however only effective as an ATP depleting agent in high dosage, since glucose and DG compete for uptake [8]. To mimic a decreased ATP:AMP ratio at a constant ATP level, cells were treated with AICAR at different concentrations. AICAR is a cell-permeable drug and its phosphorylated form ZMP structurally resembles AMP, a known activator the AMP-activated kinase (AMPK) [13].

As depicted in Figure 1A, 0.5 mM of AICAR was sufficient to down-regulate E6/E7 viral transcription in HPV-18 positive cervical carcinoma HeLa cells in a time-dependent manner. Strongest reduction was detected with 4 mM AICAR after 24 h treatment. HPV-18 suppression was selective since other reference genes such as the housekeeping gene β -actin were not affected. To demonstrate that the effect of AICAR was not merely a cell line specific phenomenon, additional HPV-16/18 positive cells were examined. CaSki cells contain approximately 500 both full length and truncated copies of HPV 16 integrated at different chromosomal locations, SW756 cells harbour multiple truncated copies of HPV-18 located at a single integration site [24]. As demonstrated in Figure 1B, both cell lines also showed a strong decrease in HPV expression, clearly indicating that AICAR treatment negatively regulates viral transcription independently of the HPV type, the copy number or the viral integration locus (Figure 1B).

Consistent with the down-regulation of HPV-18 seen on RNA level (Figure 1A), 0.5 mM AICAR treatment also leads to a selective and time-dependent reduction of the E7 oncoprotein (Figure 2). Due to the unavailability of appropriate antibodies, we could only indirectly measure the fate of the E6 oncoprotein. Figure 2 shows that in the same way as E7 and viral transcription was decreased (Figure 1A), p53 was stabilised compared to untreated control cells. Cells cultured in the presence of AICAR showed a strong decrease in UTP and CTP levels as a result of 5-phospho-D-ribosyl-1-pyrophosphate (PRPP) depletion, an important precursor for pyrimidine nucleotide synthesis [25]. To overcome pyrimidine depletion and to demonstrate that the metabolism of the treated cells was not irreversibly disturbed, HeLa cells were cultured with 0.5 mM AICAR in the presence of 20 μ M uridine. Under these conditions, the inhibitory effect on oncogene expression and stabilisation of p53

could be completely prevented (Figure 2). Conversely, at higher AICAR concentrations uridine failed to inhibit the transcriptional attenuation of HPV expression even when uridine was supplemented in concentrations up to 1 mM (data not shown).

The viral control region determines down regulation of HPV transcription. Decrease in oncogene mRNA levels can be either due to a labilization and shortening of the cytoplasmic mRNA half-life or by direct suppression of viral upstream regulatory region (URR)-directed transcriptional activity. To investigate the effect of AICAR treatment on the HPV-URR, we established a clonal subline derived from HeLa cells fused with normal human fibroblasts, which express an additional E6/E7 cDNA transcription cassette under the control of the β -actin promoter [26]. As depicted in Figure 3A, incubation with 0.5 mM AICAR only resulted in a suppression of the URR-directed E6/E7 transcription (referred to as “endo” for endogenous HPV-18 expression), while the β -actin driven viral cDNA (referred to as “exo”) was not affected. Uridine supplementation was able to abrogate the AICAR effect indicating that down-regulation of viral gene expression was regulated at the level of initiation of transcription rather than by post-transcriptional mechanisms. Additionally, to exclude any positional effect due to integration and to unequivocally demonstrate that the URR was indeed a target of the negative regulation upon AICAR treatment, HeLa cells were transfected with a HPV-18-URR luciferase reporter plasmid. H1299 cells, which contain the same reporter construct were used to monitor the effect of AICAR on the HPV-18 URR-directed transcription in HPV-negative cells. As shown in Figure 3B, in both cell lines, 4 mM AICAR treatment lead to a 6-10 times reduced luciferase activity, clearly indicating that the HPV-18-URR was target of the negative regulatory process induced by AICAR.

Selective reduction of AP-1 after AICAR treatment. HPV transcriptional activity is strongly determined by a certain set of host specific transcription factors, which bind to their cognate cis-regulatory recognition sites within the URR [27]. In the case of 2-DG it was shown that the trans-activating potential of the transcription-factor Sp1 was diminished by an increase in O-linked glycosylation [12]. Since the β -actin promoter contains numerous Sp1-like sequences [28], but was not affected upon AICAR incubation (Figure 3), we focused our attention on the transcription factor AP-1, which is known to play a central role in the transcriptional regulation of almost all HPV types investigated so far [29].

To test this notion, we examined the AP-1 binding by electrophoretic mobility shift assays (EMSA). Incubating of nuclear extracts obtained from cells treated with different

concentrations of AICAR with ^{32}P -labeled AP-1 oligonucleotides, a strong reduction of AP-1 binding could be discerned (Figure 4A). Super-shift analysis confirmed that c-Jun is the main dimerisation partner of the AP-1 complex of HeLa (Figure 4B). Monitoring the c-Jun steady state level by Westernblot, however, no quantitative reduction was detectable under conditions of low AP-1 binding (Figure 4C). These data suggest that decreased AP-1 affinity in EMSA might be the result of a post-translational modification of c-Jun, probably interfering with its affinity to DNA. To demonstrate that suppression of AP-1 binding was a selective process, EMSAs with ^{32}P -labeled Oct-1 specific oligonucleotides were carried out. In fact, under conditions where AP-1 binding was reduced (Figure 4A), both Oct-1 and Sp1 binding (data not shown) were not affected. These data clearly demonstrate that an unbalanced energy metabolism triggers a decrease of AP-1, but apparently did not impair the binding of transcription factors in general.

The effect of AICAR on the cell cycle and p53/p21^{CIP1} expression. Since viral expression is necessary to maintain a proliferative phenotype of cervical carcinoma cells [30], we examined the fate of HeLa cells at different time points after seeding in the presence of increasing concentrations of AICAR. As shown in Figure 5A, 0.5 mM AICAR completely blocked cellular growth, while at higher amounts of AICAR, the number of cells were even diminished. In fact, as revealed by phase contrast microscopy (Figure 5B), addition of 4 mM AICAR for 24 hours led to the appearance of typical apoptotic figures indicated by condensation of the cytoplasm and nuclear shrinkage (karyorhexis). In order to analyse at which phase of the cell cycle the cells became growth arrested and to quantify the extend of apoptosis, flow-cytometric analyses were performed. As depicted in Figure 5B, lower concentrations of AICAR blocked cells within S-phase, which in turn resulted in a reduced number of cells in G2/M. At 4 mM AICAR, a substantial fraction of cells (approximately 27%) accumulated in a sub-G1 position, confirming that apoptosis was taking place. At 2 mM AICAR, S-phase arrest was partially released and cell morphology changed similar to cells treated with 4 mM but without the appearance of apoptotic figures. In contrast, the HPV negative cervical carcinoma cell line C33a did not undergo apoptosis, but a reduced growth rate was observed (see supplementary data).

To get insight in the dosage effect, we monitored the expression of p53 and p21^{CIP1} at different AICAR concentrations. As shown in Figure 2, treatment with AICAR resulted in a strong increase of the p53 protein. By RT-PCR, no differences at the p53 mRNA level could be revealed (Figure 6A, upper panel), indicating that the quantitative increase of p53 was the

consequence of its reconstituted half-life due to viral oncogene suppression (Figure 1) rather than by a transcriptional effect. One major target gene involved in cell cycle control is p21^{CIP1}, an inhibitor of cyclin-dependent kinases [31]. Intriguingly, only when cellular growth arrest was accomplished, p21^{CIP1} was up-regulated, both on RNA and on protein level (Figure 6). In contrast, under conditions of apoptosis, p21^{CIP1} was not induced transcriptionally despite increased p53 protein levels. Moreover, Western blot analysis revealed that p21^{CIP1} was even not expressed, indicating that under these conditions p21^{CIP1} induction was not necessary (Figure 6B). These findings suggest that growth of HeLa can be efficiently inhibited by lower concentration of AICAR, while increasing concentrations of AICAR triggered apoptosis.

Expression of LKB1 and its role in induction of apoptosis. As already shown for cells without any HPV aetiology, AICAR also induces p53 and p21 accumulation [31]. Apparently, p53 is a direct target of activated AMPK [32], providing a novel link between cell cycle control and metabolic regulation. AMPK in turn is activated by AMPK upstream kinases (AMPKK), such as LKB1 [33]. To examine the expression of LKB1 in the context of HPV-induced carcinogenesis, we analysed the presence of the corresponding mRNA in different cervical carcinoma cells (Figure 7A). Consistent with previous results [17], HeLa cells lacked detectable LKB1 expression, while other cervical carcinoma cell lines, such as CaSki, SW756 and C33a, respectively, were found to be positive for the corresponding mRNA. Exceptions were the HPV-16 positive cervical carcinoma cell line SiHa and the tumourigenic segregant (referred to as “CGL3”) of the former non-tumourigenic somatic cell hybrid made of HeLa and primary human fibroblasts (“444”), where the conversion to tumourigenicity was obviously accompanied by a loss of LKB1 expression. The chronic myelogenous leukaemia cell line K562, known to be LKB1 positive [34] was used as a positive control for the RT-PCR reaction (Figure 7A).

As predicted recently, the absence of LKB1 and therefore the lack of AMPK activation committed cells to undergo apoptosis when they were challenged with drugs signalling low cellular energy conditions [17]. To confirm this notion, various cell lines were treated with 4 mM AICAR and programmed cell death was monitored. In fact, as depicted in Figure 7B, all cells, which lack detectable LKB1 expression showed the appearance of the PARP cleavage after AICAR treatment, characteristic for ongoing apoptosis (see also Figure 8A for HeLa cells). This suggests that LKB1-deficient cervical carcinoma cells undergo apoptosis under conditions that mimic an elevated AMP:ATP ratio.

AMPK functionality and apoptosis. In order to elucidate the activity of AMPK, phosphorylation of the downstream target acetyl-CoA-carboxylase (ACC), an enzyme involved in the fatty acid synthesis pathway, was monitored [15]. For this purpose, we chose LKB1-positive “444” cells and LKB1-negative parental HeLa cells for comparison. As demonstrated in Figure 8A, only “444” cells showed increased ACC phosphorylation, which is consistent with the presence of LKB1 expression and an activation of AMPK upon 4 mM AICAR treatment. In contrast, HeLa cells were completely refractory under the same experimental conditions, while apoptosis, as indicated by a strong PARP cleavage, was induced. To show that there still exist a redundant non-LKB1 dependent pathway activating AMPK, HeLa cells were treated with 10 μ M oligomycin, an inhibitor of mitochondrial respiration that depletes, like 2-DG, the intracellular ATP level [35]. Indeed, oligomycin activated AMPK and also led to a cleavage of PARP, while AICAR-mediated apoptosis seemed to be entirely independent from AMPK activity. Since LKB1 signalling is involved in the cellular response to low energy, we hypothesised that the presence of LKB1 should protect cells from apoptosis induced by drugs that further elevate intracellular AMP.

Taking advantage of our somatic cell hybrid model system, metabolic stress such as the application of 2-DG can be investigated both in non-malignant cells expressing LKB1 and in tumourigenic segregants derived from the very same hybrid (“CGL3”), but lacking LKB1 (see Figure 7A). As predicted, 2-DG was inducing apoptosis only in LKB1-negative cells (HeLa and “CGL3”), while “444” cells were resistant (Figure 8B).

Knock-down of LKB1 transcription by siRNA. To study the fate of AICAR treated cells after knocking-down LKB1 expression, both C33a (data not shown) and “444” hybrids were transfected with LKB1 siRNA in comparison with a siRNA directed against the luciferase gene (siLuc) as non-specific control. As shown in Figure 9A, LKB1 siRNA delivery resulted in an almost complete reduction of the corresponding mRNA, while siLuc had no effect. When cells were incubated with 4 mM AICAR for 24 hour, 100% of LKB1 knock-down cells were eradicated in contrast to siRNALuc transfected controls. To monitor the mode of cell death, incubation with AICAR was reduced to 8h, cells were stained with DAPI and SR 101 as a protein counter stain and analysed by fluorescence microscopy. As depicted in Figure 9B, LKB1 knock-down cells underwent extensive cell death (panel 10-12) in contrast to the siRNALuc controls, which showed no morphological changes (panel 4-6). Panel 12 revealed the presence of necrotic (loss of plasma integrity without morphological changes of the nuclei) rather than apoptotic cells, indicated by loss of cell integrity. This suggests that

AICAR or ATP-depleting agents may represent potential therapeutic drugs that selectively eradicate LKB1-deficient cervical carcinoma cells via apoptosis or necrosis.

DISCUSSION

A hallmark of many highly invasive tumours, including cervical cancer, is their high glycolytic rate, strongly supporting Warburg's dictum of a relationship between a glycolytic shift and malignant progression. Furthermore, a glycolytic phenotype, which guarantees constant energy supply even when oxygen levels decreased is evidently also an essential prerequisite to maintain efficient transcriptional activity of the viral oncoproteins E6 and E7 [12]. Here, not only 2-DG and limited glucose availability selectively reduce HPV expression in cervical carcinoma cells [11; 12; 36], but also AICAR (Figure 1), a known activator of AMPK, which simulates low energy condition without ATP depletion. The suppressive effect was not limited to HPV-18 positive HeLa cells, but could also be visualized in other cell lines (Figure 1), differing in their HPV type, their viral copy number and viral chromosomal localization (Figure 1B). Since both E6 and E7 transcription was down-regulated by AICAR treatment, p53 stabilisation can be explained by reduced expression of E6 (Figure 2).

Remarkably, there seems to be an evolutionary well-designed circuit between sustained HPV transcription and oncoprotein functionality, since E7 itself is capable to reprogram the metabolism of its host cell. E7 physically interacts with the M2 pyruvate kinase (M2-PK) [37] and the acid α -glucosidase [38], both key regulatory enzymes involved in the intracellular accumulation of glycolytic phosphometabolites and glycogen breakdown [11]. Binding of E7 to M2-PK, for instance, changes its catalytic property, which finally leads to an increase of nucleotide precursors required for DNA synthesis and cell growth [37]. Accordingly, for a successful virus-host interaction it is reasonable to assume that viral transcription, which continuously needs a high metabolic state for keeping up cell proliferation, is down-regulated by a negative feedback loop when the host cell is sensing low energy conditions.

As depicted in Figure 3A, we could show that AICAR exclusively affected URR-directed gene expression, while the transcriptional activity of a β -actin-driven E6/E7 transcription cassette, which contains a 3'-cellular poly-adenylation site from SW756 cells remained unchanged. The same was true, when HPV18-URR driven luciferase reporter constructs were transfected (Figure 3B), clearly supporting the notion that HPV is suppressed at the level of initiation of transcription rather than post-transcriptionally. Recently, it has been demonstrated that 2-DG, hypoglycaemia and hypoxia can affect the binding affinity of the transcription factor Sp1 by changing its glycosylation profile, which is added in a post-translational manner [12]. In our experiments AICAR treatment, however, had no effect on Sp1 (data not shown), but a decreased binding affinity of the transcription factor AP-1 could

be discerned (Figure 4A). In agreement with our finding, evidence has been provided that AICAR also interferes with AP-1 binding in other systems [39], suggesting a general functional relationship between AP-1 activity and the metabolic state of the cell.

Actually AP-1 is not only involved in various cellular regulatory processes [40], but also in the maintenance of HPV expression [29]. This notion has been confirmed by site-directed mutagenesis of the AP-1 sites within the viral enhancer/ promoter region, where in contrast to other *cis*-regulatory sequences, URR-driven transcription was almost completely abolished [27]. The finding that Oct-1 binding was not reduced under these conditions clearly demonstrated the selectivity of this process. Decreased AP-1 binding in the EMSA, however, could not be attributed to a reduction of c-Jun, the major dimerisation partner of the Jun-family members in cervical carcinoma cells (Figure 4B) [41], since Western blot analysis of nuclear extracts revealed that similar expression levels were preserved (Figure 4C). In respect of functionality it should be stressed that AICAR also causes activation of the glycogen synthase kinase-3 (GSK3) [42], which phosphorylates c-Jun at its C-terminal DNA binding domain thereby preventing DNA binding [43]. This may explain the reduced AP-1 signals in the EMSA (Figure 4A) despite unchanged amounts of c-Jun, even after longer AICAR treatment (Figure 4C). Note that GSK3 inhibitor lithium chloride (LiCl) [44] was not relieving the transcriptional block on HPV-18 transcription (data not shown). How AICAR is definitively diminishing AP-1 binding still remains to be elucidated.

Although all tested AICAR concentrations reduced HPV-18 transcription in HeLa cells to a similar extent (Figure 1), the effects on proliferation and survival differed significantly (Figure 5A). While 0.5 mM AICAR caused accumulation of cells in S-phase with a depletion of the G2/M fraction, addition of 4 mM AICAR for 24 hours led to the induction of apoptosis, which was indicated by the appearance of the characteristic sub-G1 peak after flow cytometric measurement (Figure 5B). Growth arrest at lower and moderate AICAR concentrations was in line with a post-translational increase of p53 and the induction of its major target gene p21^{CIP1}, both on RNA and on protein level (Figure 6). Elevation of p53 and inhibition of oncogene expression could be completely prevented when 0.5 mM AICAR was applied in combination with 20 μ M uridine, pointing to an inhibition of phospho-ribosyl-pyrophosphate-synthetase and nucleic acid synthesis as a further target of AICAR (Figure 2) [25]. p53 is a central protein in cell cycle control that signals either cessation of growth or induction of apoptosis, depending on the severity of cellular damage [32]. Moreover, its activity is also regulated by AMPK, demonstrating that p53 is part of a metabolic checkpoint, which determines the outcome of the biological response after energy

depletion [32]. In HepG2 cells, induction of p53 and p21^{CIP1} after AICAR treatment has been also described [31]. However, p53 was induced on transcriptional level, whereas in our case p53 was stabilised as a consequence of viral oncogene suppression (Figure 1 and 2). Note that under conditions when cells underwent apoptosis, p21^{CIP1} mRNA was not induced and the corresponding protein was not detectable (Figure 6A). This is consistent with previous reports, suggesting that p21^{CIP1} has anti-apoptotic activity [45] and can be cleaved by a caspase-like mechanism [46].

Despite the fact that AICAR is considered to be a specific inducer of AMPK [13], no phosphorylation of its downstream target ACC [15] can be detected in HeLa cells (Figure 8A). This correlates with the absence of the AMPK upstream kinase LKB1 [42] (see also Figure 7), a putative tumour suppressor gene, first described to be mutated in the rare inherited disease, the Peutz-Jeghers-syndrome [47]. Monitoring the presence of LKB1 mRNA in other cervical carcinoma cells, the picture was not uniform (Figure 7A), suggesting that loss of LKB1 expression is not a general feature of HPV-induced carcinogenesis. There is strong evidence that not AMPK itself but one of the upstream kinases (either LKB1 or the Calmodulin-dependent kinase) determine the biological outcome after AICAR treatment [17; 35]. LKB1 deficient mouse embryonic fibroblasts (MEF), for example, undergo extensive apoptosis, but not wild type cells or their heterozygous controls [17]. In HeLa cells, LKB1 seems to be not transcribed due to promotor *de novo* methylation [17], but is reconstituted upon somatic cell hybridization with normal human fibroblasts ("444"). Tumourigenic segregants derived from the same hybrids ("CGL3") have lost LKB1 expression, suggesting that progression to malignancy is paralleled by LKB1 down-regulation. Remarkably, similar to the aforementioned situation, only cells lacking LKB1 underwent cell death, while others were found to be resistant (Figure 7B and 8A). According to the model presented by Shaw et al. [17], lack of LKB1 expression should also sensitise cell to apoptosis when the ATP:AMP ratio is altered. In fact, 2-DG, which activates AMPK via the Calmodulin-dependent kinase [35] only induced apoptosis in LKB1-negative HeLa cells and "CGL3" hybrids, but not in their non-malignant, LKB1-positive counterparts (Figure 8B), clearly confirming the relationship between AICAR induced cytotoxicity and the absence of LKB1 expression.

However, apoptosis (Figure 7 and 8) is apparently not the only way to eliminate LKB1 negative cells. Knocking-down LKB1 via transient delivery of siRNA resulted in a complete eradication 24 hours after AICAR treatment. Morphological changes typical for apoptosis were absent and cells seemed to be eliminated via disruption of the cellular membrane and release of DNA (Figure 9, panel 12). In comparison to cells, which already acquired a loss of

LKB1 expression during the carcinogenic process (e.g. HeLa, CGL3), a short-term knock-down of LKB1 followed by AICAR treatment lead apparently to a different biological outcome. LKB1 deficient cells underwent apoptosis (Figure 5B and 8B), whereas siRNA mediated knock-down lead to necrotic cell death. Since the activation of AMPK by AICAR in “444” cells (Figure 8A) did correlate with survival, it can be concluded that by short-term LKB1 suppression the cells can not counteract the AICAR induced metabolic stress, resulting in extensive cytotoxicity (Figure 9B).

The susceptibility of cells lacking LKB1 to undergo cell death raises the question whether interference with energy metabolism might be an additional option to eliminate chemoresistant cancer cells by a combinatorial therapy. Several strategies combining ATP depletion and anticancer agents have been tested *in vitro* and *in vivo*. Inhibition of glycolysis by either glucose withdrawal or 2-DG application enhanced radiosensitisation [48], but also death ligand induced apoptosis [46]. Furthermore, the combination of the widely used 5-FU with AICAR induced cell death in 5-FU resistant cell lines [49]. Preliminary results from our laboratory are in line with these results showing a synergistic effect of AICAR treatment and CD95-ligand addition in the induction of apoptosis. This may open new strategies in the treatment of cervical cancer, using LKB1 expression as predictor for therapeutic success.

ACKNOWLEDGEMENTS

We thank Daniela Holland for the H1299 transfected cells, Karin Butz for the Luciferase reporter plasmid (both DKFZ, Heidelberg, Germany), Eric Stanbridge (University of Irvine, Irvine CA, U.S.A.) for the hybrid cell lines, Monika Frank-Stoehr for cell cycle analysis, Rainer Schmidt and Thomas Hofmann (all DKFZ, Heidelberg) for helpful advices and discussions. This paper is dedicated to Erich Eigenbrodt who deceased in 2004.

References

- 1 zur Hausen, H. (2002). Papillomaviruses and cancer: from basic studies to clinical application. *Nat. Rev. Cancer* **2**, 342-350.
- 2 Münger, K. and Howley, P. M. (2002). Human papillomavirus immortalization and transformation functions. *Virus Res.* **89**, 213-228.
- 3 Gatenby, R. A. and Gillies, R. J. (2004). Why do cancers have high aerobic glycolysis? *Nat. Rev. Cancer* **4**, 891-899.
- 4 Warburg, O. (1956). On respiratory impairment in cancer cells. *Science* **124**, 269-270.
- 5 Eigenbrodt, E. and Glossmann, H. (1980). Glycolysis - one of the keys to cancer? *Trends Pharmacol. Sci.* **1**, 240-245.
- 6 Mazurek, S., Boschek, C. B., Hugo, F., and Eigenbrodt, E. (2005). Pyruvate kinase type M2 and its role in tumor growth and spreading. *Semin. Cancer Biol.* **15**, 300-308.
- 7 Seyfried, T. N. and Mukherjee, P. (2005). Targeting energy metabolism in brain cancer: review and hypothesis. *Nutr. Metab (Lond)* **2**, 30.
- 8 Vrbacky, M., Krijt, J., Drahotka, Z., and Melkova, Z. (2003). Inhibitory effects of Bcl-2 on mitochondrial respiration. *Physiol Res.* **52**, 545-554.
- 9 Rattan, R., Giri, S., Singh, A. K., and Singh, I. (2005). 5-Aminoimidazole-4-carboxamide-1-beta-D-ribofuranoside inhibits cancer cell proliferation in vitro and in vivo via AMP-activated protein kinase. *J. Biol. Chem.* **280**, 39582-39593.
- 10 Swinnen, J. V., Beckers, A., Brusselmans, K., Organe, S., Segers, J., Timmermans, L., Vanderhoydonc, F., Deboel, L., Derua, R., Waelkens, E., De Schrijver, E., Van de, S. T., Noel, A., Fougelle, F., and Verhoeven, G. (2005). Mimicry of a cellular low energy status blocks tumor cell anabolism and suppresses the malignant phenotype. *Cancer Res.* **65**, 2441-2448.
- 11 Maehama, T., Patzelt, A., Lengert, M., Hutter, K. J., Kanazawa, K., Hausen, H., and Rösl, F. (1998). Selective down-regulation of human papillomavirus transcription by 2-deoxyglucose. *Int. J. Cancer* **76**, 639-646.

- 12 Kang, H. T., Ju, J. W., Cho, J. W., and Hwang, E. S. (2003). Down-regulation of Sp1 activity through modulation of O-glycosylation by treatment with a low glucose mimetic, 2-deoxyglucose. *J. Biol. Chem.* **278**, 51223-51231.
- 13 Hardie, D. G. and Hawley, S. A. (2001). AMP-activated protein kinase: the energy charge hypothesis revisited. *Bioessays* **23**, 1112-1119.
- 14 Sabina, R. L., Patterson, D., and Holmes, E. W. (1985). 5-Amino-4-imidazolecarboxamide riboside (Z-riboside) metabolism in eukaryotic cells. *J. Biol. Chem.* **260**, 6107-6114.
- 15 Luo, Z., Saha, A. K., Xiang, X., and Ruderman, N. B. (2005). AMPK, the metabolic syndrome and cancer. *Trends Pharmacol. Sci.* **26**, 69-76.
- 16 Lopez, J. M., Santidrian, A. F., Campas, C., and Gil, J. (2003). 5-Aminoimidazole-4-carboxamide riboside induces apoptosis in Jurkat cells, but the AMP-activated protein kinase is not involved. *Biochem. J.* **370**, 1027-1032.
- 17 Shaw, R. J., Kosmatka, M., Bardeesy, N., Hurley, R. L., Witters, L. A., DePinho, R. A., and Cantley, L. C. (2004). The tumor suppressor LKB1 kinase directly activates AMP-activated kinase and regulates apoptosis in response to energy stress. *Proc. Natl. Acad. Sci. U. S. A* **101**, 3329-3335.
- 18 Stanbridge, E. J. (1988). Genetic analysis of human malignancy using somatic cell hybrids and monochromosome transfer. *Cancer Surv.* **7**, 317-324.
- 19 Schreiber, E., Matthias, P., Müller, M. M., and Schaffner, W. (1989). Rapid detection of octamer binding proteins with 'mini-extracts', prepared from a small number of cells. *Nucleic Acids Res.* **17**, 6419.
- 20 Lee, W., Mitchell, P., and Tjian, R. (1987). Purified transcription factor AP-1 interacts with TPA-inducible enhancer elements. *Cell* **49**, 741-752.
- 21 Scheidereit, C., Cromlish, J. A., Gerster, T., Kawakami, K., Balmaceda, C. G., Currie, R. A., and Roeder, R. G. (1988). A human lymphoid-specific transcription factor that activates immunoglobulin genes is a homoeobox protein. *Nature* **336**, 551-557.

- 22 Stoehr, M., Vogt-Schaden, M., Knobloch, M., Vogel, R., and Futterman, G. (1978). Evaluation of eight fluorochrome combinations for simultaneous DNA-protein flow analyses. *Stain Technol.* **53**, 205-215.
- 23 Dean, P. N. and Jett, J. H. (1974). Mathematical analysis of DNA distributions derived from flow microfluorometry. *J. Cell Biol.* **60**, 523-527.
- 24 Mincheva, A., Gissmann, L., and zur Hausen, H. (1987). Chromosomal integration sites of human papillomavirus DNA in three cervical cancer cell lines mapped by in situ hybridization. *Med. Microbiol. Immunol. (Berl)* **176**, 245-256.
- 25 Thomas, C. B., Meade, J. C., and Holmes, E. W. (1981). Aminoimidazole carboxamide ribonucleoside toxicity: a model for study of pyrimidine starvation. *J. Cell Physiol* **107**, 335-344.
- 26 Bachmann, A., Hanke, B., Zawatzky, R., Soto, U., van Riggelen, J., zur Hausen, H., and Rösl, F. (2002). Disturbance of tumor necrosis factor alpha-mediated beta interferon signaling in cervical carcinoma cells. *J. Virol.* **76**, 280-291.
- 27 Butz, K. and Hoppe-Seyler, F. (1993). Transcriptional control of human papillomavirus (HPV) oncogene expression: composition of the HPV type 18 upstream regulatory region. *J. Virol.* **67**, 6476-6486.
- 28 Quitschke, W. W., Lin, Z. Y., DePonti-Zilli, L., and Paterson, B. M. (1989). The beta actin promoter. High levels of transcription depend upon a CCAAT binding factor. *J. Biol. Chem.* **264**, 9539-9546.
- 29 Rösl, F. and Schwarz E (1997). Regulation of E6 and E7 oncogene transcription. In: *Papillomaviruses in Human Cancer* (Tommasino, M., Ed.), Springer Verlag, Heidelberg, 25-70
- 30 von Knebel-Döberitz, M., Oltersdorf, T., Schwarz, E., and Gissmann, L. (1988). Correlation of modified human papilloma virus early gene expression with altered growth properties in C4-1 cervical carcinoma cells. *Cancer Res.* **48**, 3780-3786.
- 31 Imamura, K., Ogura, T., Kishimoto, A., Kaminishi, M., and Esumi, H. (2001). Cell cycle regulation via p53 phosphorylation by a 5'-AMP activated protein kinase activator,

- 5-aminoimidazole- 4-carboxamide-1-beta-D-ribofuranoside, in a human hepatocellular carcinoma cell line. *Biochem. Biophys. Res. Commun.* **287**, 562-567.
- 32 Jones, R. G., Plas, D. R., Kubek, S., Buzzai, M., Mu, J., Xu, Y., Birnbaum, M. J., and Thompson, C. B. (2005). AMP-activated protein kinase induces a p53-dependent metabolic checkpoint. *Mol. Cell* **18**, 283-293.
- 33 Kyriakis, J. M. (2003). At the crossroads: AMP-activated kinase and the LKB1 tumor suppressor link cell proliferation to metabolic regulation. *J. Biol.* **2**, 26.
- 34 Tiainen, M., Ylikorkala, A. and Makela, T.P. (1999). Growth suppression by Lkb1 is mediated by a G(1) cell cycle arrest. *Proc. Natl. Acad. Sci. U. S. A* **66**, 9248-9251.
- 35 Hurley, R. L., Anderson, K. A., Franzone, J. M., Kemp, B. E., Means, A. R., and Witters, L. A. (2005). The Ca²⁺/calmodulin-dependent protein kinase kinases are AMP-activated protein kinase kinases. *J. Biol. Chem.* **280**, 29060-29066.
- 36 Kang, H. T. and Hwang, E. S. (2006). 2-Deoxyglucose: an anticancer and antiviral therapeutic, but not any more a low glucose mimetic. *Life Sci.* **78**, 1392-1399.
- 37 Zwerschke, W., Mazurek, S., Massimi, P., Banks, L., Eigenbrodt, E., and Jansen-Dürr, P. (1999). Modulation of type M2 pyruvate kinase activity by the human papillomavirus type 16 E7 oncoprotein. *Proc. Natl. Acad. Sci. U. S. A* **96**, 1291-1296.
- 38 Zwerschke, W., Mannhardt, B., Massimi, P., Nauenburg, S., Pim, D., Nickel, W., Banks, L., Reuser, A. J., and Jansen-Dürr, P. (2000). Allosteric activation of acid alpha-glucosidase by the human papillomavirus E7 protein. *J. Biol. Chem.* **275**, 9534-9541.
- 39 Weigert, C., Sauer, U., Brodbeck, K., Pfeiffer, A., Haring, H. U., and Schleicher, E. D. (2000). AP-1 proteins mediate hyperglycemia-induced activation of the human TGF-beta1 promoter in mesangial cells. *J. Am. Soc. Nephrol.* **11**, 2007-2016.
- 40 Eferl, R. and Wagner, E. F. (2003). AP-1: a double-edged sword in tumorigenesis. *Nat. Rev. Cancer* **3**, 859-868.
- 41 Soto, U., Das, B. C., Lengert, M., Finzer, P., zur Hausen, H., and Rösl, F. (1999). Conversion of HPV 18 positive non-tumourigenic HeLa-fibroblast hybrids to invasive growth involves loss of TNF-alpha mediated repression of viral transcription and modification of the AP-1 transcription complex. *Oncogene* **18**, 3187-3198.

- 42 King, T. D., Song, L., and Jope, R. S. (2006). AMP-activated protein kinase (AMPK) activating agents cause dephosphorylation of Akt and glycogen synthase kinase-3. *Biochem. Pharmacol.* **71**, 1637-1647.
- 43 Boyle, W. J., Smeal, T., Defize, L. H., Angel, P., Woodgett, J. R., Karin, M., and Hunter, T. (1991). Activation of protein kinase C decreases phosphorylation of c-Jun at sites that negatively regulate its DNA-binding activity. *Cell* **64**, 573-584.
- 44 Stambolic, V., Ruel, L., and Woodgett, J. R. (1996). Lithium inhibits glycogen synthase kinase-3 activity and mimics wingless signalling in intact cells. *Curr. Biol.* **6**, 1664-1668.
- 45 Chan, T. A., Hwang, P. M., Hermeking, H., Kinzler, K. W., and Vogelstein, B. (2000). Cooperative effects of genes controlling the G(2)/M checkpoint. *Genes Dev.* **14**, 1584-1588.
- 46 Munoz-Pinedo, C., Ruiz-Ruiz, C., Ruiz, d. A., Palacios, C., and Lopez-Rivas, A. (2003). Inhibition of glucose metabolism sensitizes tumor cells to death receptor-triggered apoptosis through enhancement of death-inducing signaling complex formation and apical procaspase-8 processing. *J. Biol. Chem.* **278**, 12759-12768.
- 47 Alessi, D. R., Sakamoto, K., and Bayascas, J. R. (2006). LKB1-Dependent Signaling Pathways. *Annu. Rev. Biochem.*
- 48 Lin, X., Zhang, F., Bradbury, C. M., Kaushal, A., Li, L., Spitz, D. R., Aft, R. L., and Gius, D. (2003). 2-Deoxy-D-glucose-induced cytotoxicity and radiosensitization in tumor cells is mediated via disruptions in thiol metabolism. *Cancer Res.* **63**, 3413-3417
- 49 Hwang, J. T., Ha, J., and Park, O. J. (2005). Combination of 5-fluorouracil and genistein induces apoptosis synergistically in chemo-resistant cancer cells through the modulation of AMPK and COX-2 signaling pathways. *Biochem. Biophys. Res. Commun.* **332**, 433-440.

Figure legends

Figure 1: Selective down-regulation of HPV-transcription in cervical carcinoma cells after treatment with AICAR. Northern blots of different cervical cancer cell lines treated with AICAR. **(A)** HPV-18 positive HeLa cells were incubated for the times indicated with different concentrations of AICAR. **(B)** RNA obtained from HPV 16-positive CaSki cells (left) and HPV 18-positive SW756 cells (right) after treatment with 0.5 mM AICAR for different periods of time. For Northern blot, 5 µg/lane of total RNA was separated under non-denaturing conditions in 1 % agarose gels. After transfer, the membranes were consecutively hybridized with HPV-16/-18 and β-actin specific DNA probes. The positions of the 28S and 18S rRNA in the ethidium stained agarose gels are indicated. (-): untreated control.

Figure 2: Reciprocal regulation of E7 and p53 after AICAR treatment – abrogation of the AICAR effect by uridine. HeLa cells were treated with 0.5 mM AICAR for different periods of time with and without supplementation of 20 µM uridine. Immunoblots were performed using antibodies raised against HPV-18 E7 and p53. Equal loading and protein transfer were confirmed by incubating the filter with an anti-actin-specific antibody. (-): untreated control.

Figure 3: Upstream regulatory region (URR)-mediated down-regulation of viral transcription after AICAR treatment. **(A)** “444” cells expressing an additional E6/E7 transcription cassette under the control of the β-actin promoter were treated with 0.5 mM AICAR with and without supplementation of 20 µM uridine for the times indicated. 5µg/lane of total RNA was separated under non-denaturing conditions in a 1 % agarose gel and the same filters were consecutively hybridised with HPV-18 and β-actin specific DNA probes. The positions of the 28S and 18S rRNA are indicated in the ethidium stained agarose gels. (-): untreated control. **(B)** Luciferase reporter assay with HeLa and H1299 cells carrying the luciferase reporter construct under the control of HPV-18 URR. Semi-stably transfected cells were treated with 4 mM AICAR for 24 h and luciferase activity was compared with untreated controls. Ordinate: renilla luciferase units per µg total cellular protein (RLU/µg).

Figure 4: Selective reduction of AP-1 binding after AICAR treatment. **(A)** Electromobility shift assay (EMSA): nuclear extracts obtained from treated and non-treated cells were incubated with ³²P-labelled oligonucleotides specific for AP-1 or Oct-1. The incubation

time and the AICAR concentrations are indicated. **(B)** Supershifts showing the main components in the AP-1 complex of HeLa cells. The shifted bands are indicated by arrows. **(C)** Nuclear protein extracts were used for immunoblots with a c-Jun specific antibody. Equal loading and protein transfer were confirmed by incubating the same filter with an anti-actin-specific antibody.

Figure 5: Growth curves and cell cycle analysis after AICAR treatment. **(A)** Follow-up of the cellular growth of 1×10^4 HeLa cells 1-4 days in the presence of AICAR. Ordinate: number of cells ($\times 10^5$), abscissa: different concentrations of AICAR. **(B)** Representative flow cytometric profiles and the corresponding morphology of HeLa cells after incubation with AICAR. The percentage of cells present in the different phases of the cell cycle (G1, S, G2/M) as well as the percentage of apoptotic cells (reflected by the sub-G1 peak) are given in the table below and represent the mean of three different experiments. Magnification of the phase-contrast micrographs: 200 x.

Figure 6: Dosage effect of AICAR on p53 and p21^{CIP1} expression. **(A)** RNAs of AICAR treated cells were reverse transcribed. RT-PCR products of p53, p21^{CIP1} and GAPDH after separation in a 1% agarose gel. (Contr.): untreated cells. **(B)** Immunoblot of total protein extracts with antibodies against p53 and p21^{CIP1}. Equal loading and protein transfer were confirmed by incubating the same filter with an anti-actin-specific antibody.

Figure 7: LKB1 expression and apoptosis. **(A)** RNAs from different cervical carcinoma cell lines and derived somatic cell hybrids were reverse transcribed and the RT-PCR products of LKB1 and GAPDH were separated in a 1% agarose gel. **(B)** The indicated cell lines were treated for 24 h with 4 mM AICAR. For immunoblot, total protein extracts were incubated with antibodies against PARP and actin. The arrow indicates the PARP cleavage product.

Figure 8: Absence of LKB1 activity in HeLa cells, but not in non-malignant somatic cell hybrids - selective induction of apoptosis by 2-deoxyglucose in LKB-1 negative cells. **(A)** HeLa and “444” cells were treated for 24 h with 0.5 and 4 mM AICAR or 10 μ M oligomycin, respectively. Total protein extracts were used for Western blot analysis to monitor the phosphorylation of the AMPK downstream substrate ACC (P-ACC) and cleavage of PARP. Actin was again used as a loading and transfer control. **(B)** Indicated cell lines were treated with 45 mM 2-DG for different periods of time and total protein extracts were used for

immunoblots. Filters were incubated with antibodies against PARP and actin, the latter for loading control.

Figure 9: Knock-out of LKB1 transcription by siRNA. “444” cells were transfected in triplicate with siRNA against LKB1 and against luciferase as negative control. After 24 h cells were split 1:4 and 60 h post transfection, RNA from one of the plates was extracted. **(A)** For RT-PCR, LKB1 specific primers and GAPDH primers as internal control were used. AICAR treatment was started 60 h post transfection. **(B)** After 8 h treatment, cells were harvested, prepared and stained for fluorescence microscopy. “444” cells transfected with siRNA against luciferase under control conditions (1-3) and after 8 h 4 mM AICAR treatment (4-6). Untreated LKB1 knock-down cells (7-9) and after 8 h 4 mM AICAR treatment (10-12). Magnification: 200 x.

Figure 1

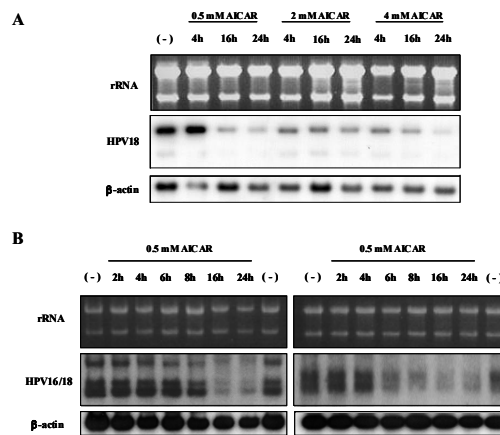


Figure 2

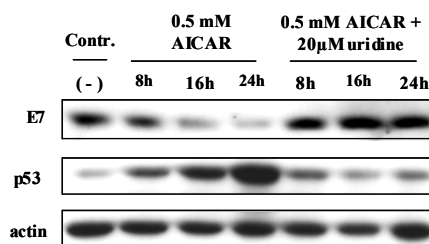


Figure 3

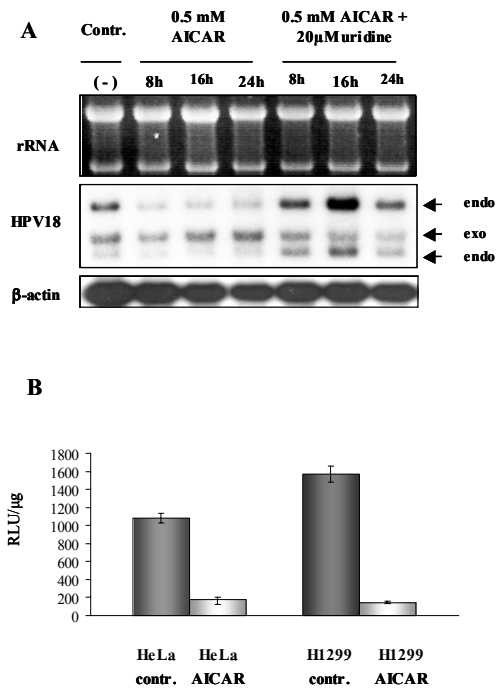


Figure 4

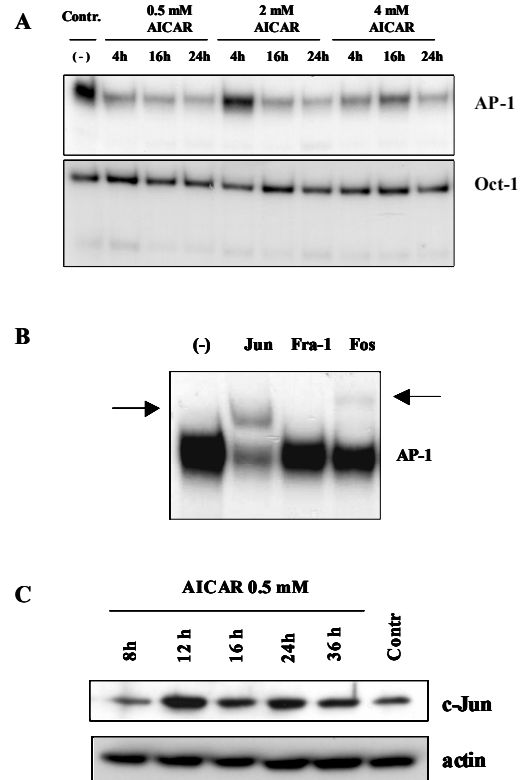
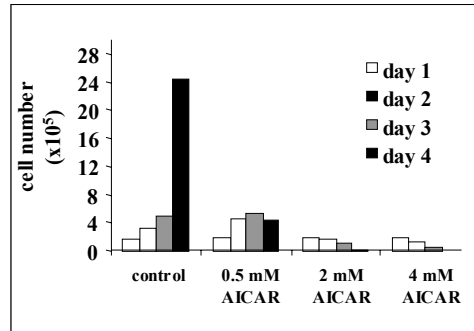


Figure 5

A



B

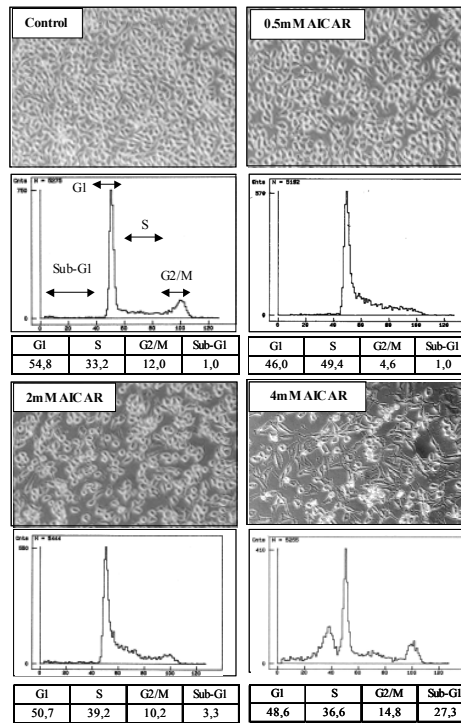


Figure 6

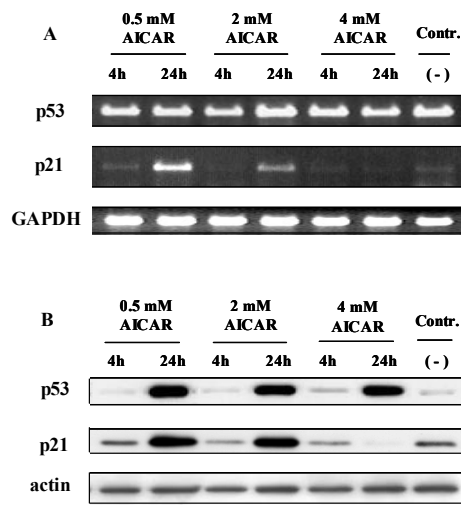


Figure 7

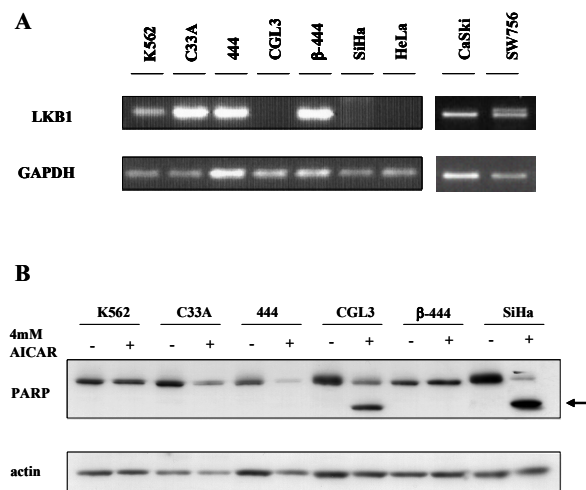


Figure 8

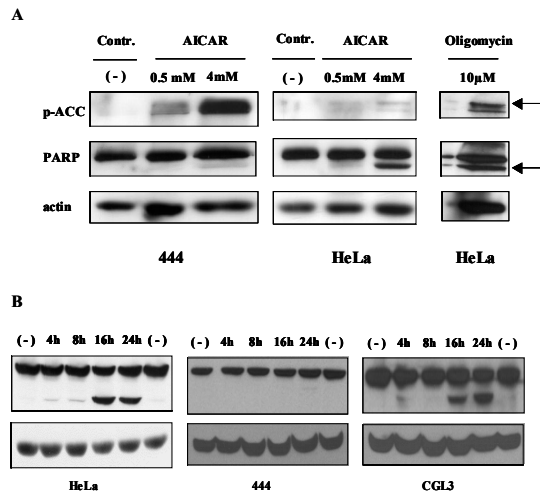


Figure 9

